

NCKU-HEP-97-04

Unified derivation of evolution equations

Hsiang-nan Li

Department of Physics, National Cheng-Kung University,
Tainan, Taiwan, Republic of China

PACS numbers: 12.38.Cy, 11.10.Hi

Abstract

We derive the evolution equations of parton distribution functions appropriate in different kinematic regions in a unified and simple way using the resummation technique. They include the Dokshitzer-Gribov-Lipatov-Altarelli-Parisi equation for large momentum transfer Q , the Balitskii-Fadin-Kuraev-Lipatov equation for a small Bjorken variable x , and the Ciafaloni-Catani-Fiorani-Marchesini equation which embodies the above two equations. The relation among these equations is explored, and possible applications of our approach are proposed.

I. INTRODUCTION

Perturbative QCD (PQCD), as a gauge field theory, involves large logarithms from radiative corrections at each order of the coupling constant α_s , such as $\ln Q$ in the kinematic region with a large momentum transfer Q and $\ln(1/x)$ in the region with a small Bjorken variable x . These logarithms, spoiling the perturbative expansion, must be organized. To organize the logarithmic corrections to a parton distribution function, the various evolution equations have been derived. For example, the Dokshitzer-Gribov-Lipatov-Altarelli-Parisi (DGLAP) equation [1] sums single logarithms $\ln Q$ for a large x , the Balitskii-Fadin-Kuraev-Lipatov (BFKL) equation [2] sums $\ln(1/x)$ for a small x , and the Ciafaloni-Catani-Fiorani-Marchesini (CCFM) equation [3], appropriate for both large and small x , unifies the above two equations. The conventional derivation of the evolution equations usually requires complicated diagrammatic analyses. The idea is to locate the region of the loop momenta flowing through the rungs (radiative gluons) of a ladder diagram, in which leading logarithmic corrections are produced, and to sum the ladder diagrams to all orders. For the DGLAP, BFKL, and CCFM equations, the important regions are those with the strong transverse momentum ordering, the strong rapidity ordering, and the strong angular ordering, respectively.

In this paper we shall propose an alternative approach to the all-order summations of the various large logarithms. This approach is based on the Collins-Soper-Sterman resummation technique, which was developed originally for the organization of double logarithms $\ln^2 Q$ [4]. Recently, we applied this technique to some hard QCD processes, such as deep inelastic scattering, Drell-Yan production, and inclusive heavy meson decays, and demonstrated how to resum the double logarithms contained in parton distribution functions into Sudakov form factors [5]. It has been shown [5, 6] that the resummation technique is equivalent to the Wilson-loop formalism [7, 8, 9] for the summation of soft logarithms. Here we shall further show that it can also deal with the single-logarithm cases, *i.e.*, the evolution equations mentioned above. Therefore, the resummation technique indeed has a wide application in PQCD. It will be found that our approach is much simpler than the conventional one, and provides a unified viewpoint to the evolution equations.

The procedures of resummation are summarized below. The derivative of a parton distribution function with respect to Q or x is first related to

a new function, which contains a special gluon vertex. This relation, as a consequence of the Ward identity, is exact. Factorizing the new function into the convolution of the subdiagram involving the special vertex with the original parton distribution function, we derive the evolution equation. At this stage, the kinematic orderings of radiative gluons are specified, and the subdiagram is identified as the corresponding kernels. We show explicitly that the lowest-order subdiagram gives the kernel for the leading-logarithm summation.

In the region with both large Q and small x many gluons are radiated in scattering processes with small spatial separation among them, and a new effect from the annihilation of two gluons into one gluon becomes important. Taking into account this effect, a nonlinear evolution equation, the Gribov-Levin-Ryskin (GLR) equation [10] is obtained. Using the resummation technique, the annihilation effect is introduced through next-to-leading-twist contributions to the subdiagram containing the special vertex, and the GLR equation can be derived easily [11]. In the present work we shall not address this subject, because it is not very relevant.

We derive the DGLAP, BFKL and CCFM equations in Sect. II, III, and IV, respectively, by means of the resummation technique in axial gauge. We explain how the subdiagram containing the special vertex reduces to the evolution kernels in the different kinematic regions. Section V is the conclusion.

II. THE DGLAP EQUATION

Consider deep inelastic scattering (DIS) of a hadron with a light-like momentum $p = p^+ \delta^{\mu+}$ in the large x limit, where $x = -q^2/(2p \cdot q) = Q^2/(2p \cdot q)$ is the Bjorken variable with q the momentum transfer to the hadron through a virtual photon. According to factorization theorems, collinear divergences arising from radiative corrections to DIS are absorbed into a quark distribution function $\phi(\xi, p^+)$ associated with the hadron, ξ being the momentum fraction of a parton. The argument p^+ denotes the large logarithms $\ln p^+$ from the collinear divergences, which will be organized.

In the axial gauge $n \cdot A = A^+ = 0$, $n^\mu = \delta^{\mu-}$ being a vector on the light cone, the gauge invariant distribution function ϕ is defined, in the modified

minimum subtraction scheme, by

$$\phi(\xi, p^+) = \int \frac{dy^-}{2\pi} e^{-i\xi p^+ y^-} \frac{1}{2} \sum_{\sigma} \langle p, \sigma | \bar{q}(y^-) \frac{1}{2} \gamma^+ q(0) | p, \sigma \rangle |_{A^+=0}, \quad (1)$$

where γ^+ is a Dirac matrix, and $|p, \sigma\rangle$ denotes the incoming hadron with momentum p and spin σ . An average over color is understood. To implement the resummation technique, we allow n to vary away from the light cone (*i.e.*, $n^2 \neq 0$) temporarily, and the resultant n -dependent distribution function is written as

$$\phi^{(n)}(\xi, p^+) = \int \frac{dy^-}{2\pi} e^{-i\xi p^+ y^-} \frac{1}{2} \sum_{\sigma} \langle p, \sigma | \bar{q}(y^-) \frac{1}{2} \gamma^+ q(0) | p, \sigma \rangle |_{n \cdot A=0}. \quad (2)$$

The above formula is similar to the definition for a quark decay function employed in [4]. After deriving the evolution equation, we let n^ν approach $\delta^{\mu-}$, and $\phi^{(n)}$ coincides with ϕ in Eq. (1). That is, the arbitrary vector n appears only at the intermediate stage of our formalism, and as an auxiliary tool of the resummation technique. $\phi^{(n)}$ can be expressed as the convolution of an infrared finite function with ϕ , and thus they contain the same nonperturbative information. Their relation will be investigated in details elsewhere [12].

The key step of resummation is to obtain the derivative $p^+ d\phi^{(n)}/dp^+$. Because of the scale invariance of $\phi^{(n)}$ in the vector n as indicated by the gluon propagator, $-iN^{\mu\nu}(l)/l^2$, with

$$N^{\mu\nu} = g^{\mu\nu} - \frac{n^\mu l^\nu + n^\nu l^\mu}{n \cdot l} + n^2 \frac{l^\mu l^\nu}{(n \cdot l)^2}, \quad (3)$$

$\phi^{(n)}$ must depend on p^+ via the ratio $(p \cdot n)^2/n^2$. Hence, we have the chain rule relating $p^+ d/dp^+$ to d/dn [4]:

$$p^+ \frac{d}{dp^+} \phi^{(n)} = - \frac{n^2}{v \cdot n} v_\alpha \frac{d}{dn_\alpha} \phi^{(n)}, \quad (4)$$

with $v_\alpha = \delta_{\alpha+}$ a vector along p . The operator d/dn_α applies only to the gluon propagator, giving [4]

$$\frac{d}{dn_\alpha} N^{\mu\nu} = - \frac{1}{n \cdot l} (l^\mu N^{\alpha\nu} + l^\nu N^{\mu\alpha}). \quad (5)$$

Since p flows through both quark and gluon lines, while n appears only in gluon lines, the analysis is simplified by considering the derivative with respect to n , instead of p^+ .

The loop momentum l^μ (l^ν) carried by the differentiated gluon contracts with a vertex in $\phi^{(n)}$, which is then replaced by a special vertex [4]

$$\hat{v}_\alpha = \frac{n^2 v_\alpha}{v \cdot n n \cdot l} . \quad (6)$$

This special vertex can be simply read off the combination of Eqs. (4) and (5). The contraction of l^μ (l^ν) leads to the Ward identities,

$$\frac{i(\not{k} + \not{l})}{(k+l)^2} (-i \not{l}) \frac{i \not{k}}{k^2} = \frac{i \not{k}}{k^2} - \frac{i(\not{k} + \not{l})}{(k+l)^2} , \quad (7)$$

for a quark-gluon vertex, and

$$l^\nu \frac{-i N^{\alpha\mu}(k+l)}{(k+l)^2} \Gamma_{\mu\nu\lambda} \frac{-i N^{\lambda\gamma}(k)}{k^2} = -i \left[\frac{-i N^{\alpha\gamma}(k)}{k^2} - \frac{-i N^{\alpha\gamma}(k+l)}{(k+l)^2} \right] , \quad (8)$$

for the triple-gluon vertex $\Gamma_{\mu\nu\lambda}$. The Ward identity for the four-gluon vertex,

$$\begin{aligned} \Gamma_{\lambda\mu\nu\sigma}^{abcd} \propto & f^{abe} f^{cde} (g_{\lambda\nu} g_{\mu\sigma} - g_{\lambda\sigma} g_{\mu\nu}) + f^{ace} f^{bde} (g_{\lambda\mu} g_{\nu\sigma} - g_{\lambda\sigma} g_{\mu\nu}) \\ & + f^{ade} f^{cbe} (g_{\lambda\nu} g_{\mu\sigma} - g_{\lambda\mu} g_{\sigma\nu}) , \end{aligned} \quad (9)$$

is simpler. The sum of the four contractions from l_1^λ , l_2^μ , l_3^ν , and l_4^σ to the four-gluon vertex vanishes: The contractions from l_1^λ and l_2^μ to the first term of $\Gamma_{\lambda\mu\nu\sigma}^{abcd}$ cancel each other, because the first term is antisymmetric with respect to the interchange of the indices λ and μ . Similar cancellation occurs between the contractions from l_3^ν and l_4^σ . The contractions from l_1^λ and l_3^ν and from l_2^μ and l_4^σ to the second term cancel separately. The contractions from l_1^λ and l_4^σ and from l_2^μ and l_3^ν to the third term also cancel separately.

Summing all the diagrams with different differentiated gluons, those embedding the special vertices cancel by pairs, leaving the one in which the special vertex moves to the outer end of the quark line [4]. For a fixed x , we obtain the formula,

$$p^+ \frac{d}{dp^+} \phi^{(n)}(x, p^+) = 2 \bar{\phi}(x, p^+) , \quad (10)$$

shown in Fig. 1(a), where $\bar{\phi}$, the new function mentioned in the Introduction, contains one special vertex represented by a square. An identical formula to Eq. (10) has been derived for a quark decay function in [4]. The coefficient 2 comes from the equality of the new functions with the special vertex on either of the two valence quark lines. Equation (10) is an exact consequence of the Ward identity without any approximation [4]. An approximation will be introduced, when relating $\bar{\phi}$ to $\phi^{(n)}$ by factorizing out the subdiagram containing the special vertex, such that Eq. (10) becomes a differential equation of $\phi^{(n)}$.

It is known that factorization holds only in important regions. The important regions of the loop momentum flowing through the special vertex are soft and hard, since the vector n does not lie on the light cone, and the collinear enhancements are suppressed. In the soft and hard regions $\bar{\phi}$ can be factorized into the convolution of the subdiagram containing the special vertex with the original distribution function $\phi^{(n)}$,

$$\begin{aligned} \bar{\phi}_s(x, p^+) &= ig^2 \mathcal{C}_F \mu^\epsilon \int \frac{d^{4-\epsilon} l}{(2\pi)^{4-\epsilon}} \frac{\hat{v}_\mu v_\nu}{v \cdot l} N^{\mu\nu}(l) \left[\frac{1}{l^2} \phi^{(n)}(x, p^+) \right. \\ &\quad \left. + 2\pi i \delta(l^2) \phi^{(n)}(x + l^+/p^+, p^+) \right] - \delta K \phi^{(n)}(x, p^+) , \end{aligned} \quad (11)$$

$$\begin{aligned} \bar{\phi}_h(x, p^+) &= -ig^2 \mathcal{C}_F \mu^\epsilon \int \frac{d^{4-\epsilon} l}{(2\pi)^{4-\epsilon}} \hat{v}_\mu \frac{N^{\mu\nu}(l)}{l^2} \left[\frac{\xi \not{p} - \not{l}}{(\xi p - l)^2} \gamma_\nu + \frac{v_\nu}{v \cdot l} \right] \phi^{(n)}(x, p^+) \\ &\quad - \delta G \phi^{(n)}(x, p^+) , \end{aligned} \quad (12)$$

where $\mathcal{C}_F = 4/3$ is the color factor, and δK and δG are additive counterterms. The function $\bar{\phi}_s$, absorbing the soft divergences of the subdiagram, corresponds to Fig. 1(b), where the eikonal approximation for the valence quark propagator has been made. The eikonal propagator is represented by a double line in the figure. The first and second terms in the integral are associated with the virtual and real gluon emissions, respectively, where $\phi^{(n)}(x + l^+/p^+, p^+)$ implies that the parton coming out of the hadron carries the longitudinal momentum $x p^+ + l^+$ in order to radiate a real gluon of momentum l^+ . The function $\bar{\phi}_h$, absorbing the ultraviolet divergences, corresponds to Fig. 1(c), where the subtraction of the second diagram ensures that the involved loop momentum is hard. We emphasize that the factorization formulas in Eqs. (11) and (12) are not exact, but hold only up to the leading logarithms $\ln p^+$.

Employing the variable change $\xi = x + l^+/p^+$, and performing the integrations in Eqs. (11) and (12) straightforwardly, we arrive at

$$\begin{aligned}\bar{\phi}(x, p^+) &= \bar{\phi}_s(x, p^+) + \bar{\phi}_h(x, p^+) \\ &= \int_x^1 d\xi \left[K(x, \xi, p^+, \mu) + G(x, \xi, p^+, \mu) \right] \phi^{(n)}(\xi, p^+) ,\end{aligned}\quad (13)$$

with

$$\begin{aligned}K &= \frac{\alpha_s(\mu)}{\pi\xi} \mathcal{C}_F \left[\frac{1}{(1-x/\xi)_+} + \ln \frac{\nu p^+}{\mu} \delta(1-x/\xi) \right] , \\ G &= -\frac{\alpha_s(\mu)}{\pi\xi} \mathcal{C}_F \ln \frac{\xi \nu p^+}{\mu} \delta(1-x/\xi) ,\end{aligned}\quad (14)$$

where constants of order unity have been dropped, and $\nu = \sqrt{(v \cdot n)^2/|n^2|}$ is the gauge factor. Equation (14) confirms our argument that $\phi^{(n)}$ depends on p and n through the ratio $(p \cdot n)^2/n^2 = (\nu p^+)^2$. In the region with $x \rightarrow 1$ the logarithm $\ln(\xi \nu p^+/\mu)$ in G can be replaced by $\ln(\nu p^+/\mu)$.

We then treat K and G by renormalization group (RG) methods:

$$\mu \frac{d}{d\mu} K = -\lambda_K = -\mu \frac{d}{d\mu} G . \quad (15)$$

The anomalous dimension of K is defined by $\lambda_K = -\mu d\delta K/d\mu$, whose explicit expression is not essential here. When solving Eq. (15), we allow the variable μ to evolve from the scale of K to the scale of G . The RG solution of $K + G$ is given by

$$\begin{aligned}K(x, \xi, p^+, \mu) + G(x, \xi, p^+, \mu) &= K(x, \xi, p^+, p^+) + G(x, \xi, p^+, p^+) \\ &\quad - \int_{p^+}^{p^+} \frac{d\bar{\mu}}{\bar{\mu}} \lambda_K(\alpha_s(\bar{\mu})) , \\ &= \frac{\alpha_s(p^+)}{\pi\xi} \mathcal{C}_F \frac{1}{(1-x/\xi)_+} ,\end{aligned}\quad (16)$$

where the initial conditions $K(x, \xi, p^+, p^+)$ and $G(x, \xi, p^+, p^+)$ do not contain large logarithms after choosing μ as p^+ . Note that the gauge factor ν cancels between K and G , implying the gauge invariance of the evolution kernel $K + G$.

A remark is in order. The source of double logarithms, *i.e.*, the integral containing λ_K , vanishes as shown in Eq. (16). If the transverse degrees of freedom of a parton are included, an extra factor $\exp(i\mathbf{l}_T \cdot \mathbf{b})$, b being the conjugate variable of the transverse momentum k_T carried by the parton, will be associated with the real gluon emission [4, 5]. Then we deal with a two-scale problem. Approximating $\phi^{(n)}(x + l^+/p^+, k_T, p^+)$ by $\phi^{(n)}(x, k_T, p^+)$, the integration over l^+ can also be performed, and the convolution in Eq. (13) is simplified to a multiplication in the b space,

$$\bar{\phi}(x, b, p^+) = [K(x, b, \mu) + G(x, p^+, \mu)] \phi^{(n)}(x, b, p^+) , \quad (17)$$

with [5]

$$K(x, b, \mu) = \frac{\alpha_s(\mu)}{\pi} \mathcal{C}_F \ln \frac{1}{b\mu} . \quad (18)$$

Hence, K is characterized by the smaller scale $1/b$, and μ should be set to $1/b$ in order to minimize the large logarithms. Consequently, $1/b$ is substituted for the lower bound of $\bar{\mu}$ in Eq. (16), and double logarithms exist. This is the difference between this work and [4]. The above discussion indicates that the resummation technique is applicable to the single-logarithm as well as double-logarithm cases.

Inserting Eq. (16) into (13), Eq. (10) becomes

$$p^+ \frac{d}{dp^+} \phi^{(n)}(x, p^+) = \frac{\alpha_s(p^+)}{\pi} \int_x^1 \frac{d\xi}{\xi} P(x/\xi) \phi^{(n)}(\xi, p^+) , \quad (19)$$

with the kernel

$$P(z) = \mathcal{C}_F \frac{2}{(1-z)_+} . \quad (20)$$

Now we make n^μ approach $\delta^{\mu-}$ (the light cone), and obtain

$$Q \frac{d}{dQ} \phi(x, Q) = \frac{\alpha_s(Q)}{\pi} \int_x^1 \frac{d\xi}{\xi} P(x/\xi) \phi(\xi, Q) , \quad (21)$$

where the variable p^+ has been replaced by Q , and the gauge invariance of the distribution function is restored. It is easy to identify P as the splitting function P_{qq} in the limit $z \rightarrow 1$,

$$P_{qq}(z) = \mathcal{C}_F \frac{1+z^2}{(1-z)_+} . \quad (22)$$

Hence, Eq. (10) leads to the DGLAP equation (21), and the diagrams in Fig. 1(b) give the splitting function.

Note that only the term of P_{qq} singular at $z \rightarrow 1$, *i.e.*, $\xi \rightarrow x$, is reproduced in the resummation approach. The reason is as follows. The z^2 term in the numerator of P_{qq} arises from the radiative correction with the ends of a real gluon attaching each valence quark line, whose loop integral is written as

$$I = g^2 \mathcal{C}_F \int \frac{d^4 l}{(2\pi)^4} \text{Tr} \left[\gamma_\mu \frac{\xi \not{p} - \not{l}}{(\xi p - l)^2} \frac{\gamma^+}{2} \frac{\xi \not{p} - \not{l}}{(\xi p - l)^2} \gamma_\nu \not{p} \right] \times N^{\mu\nu}(l) 2\pi \delta(l^2) \delta \left(\xi - x - \frac{l^+}{p^+} \right). \quad (23)$$

\not{p} in the trace comes from the Dirac structure of the proton distribution function. The numerator $\xi \not{p} - \not{l}$ contributes the factor $\xi p^+ - l^+ = x p^+$ because of the last δ function. The denominator $(\xi p - l)^2 = -2\xi p^+ v \cdot l$ gives the factor ξp^+ due to the on-shell gluon with $l^2 = 0$. Their combination leads to a power of $z = x/\xi$. The two fermion propagators then explain the term z^2 .

When applying the derivative in Eq. (4) to $N^{\mu\nu}$, we have Eq. (5), whose first term renders Eq. (23) reduce to

$$I = -g^2 \mathcal{C}_F \int \frac{d^4 l}{(2\pi)^4} \text{Tr} \left[\frac{\gamma^+}{2} \frac{\xi \not{p} - \not{l}}{(\xi p - l)^2} \gamma_\nu \not{p} \right] \times \hat{v}_\alpha N^{\alpha\nu}(l) 2\pi \delta(l^2) \delta \left(\xi - x - \frac{l^+}{p^+} \right), \quad (24)$$

as described by Fig. 2. To obtain the above expression, we have used

$$\not{l} \frac{\xi \not{p} - \not{l}}{(\xi p - l)^2} = \frac{\xi \not{l} \not{p}}{-2\xi p^+ v \cdot l} = -1 + \frac{\xi \not{p} \not{l}}{2\xi p^+ v \cdot l}, \quad (25)$$

where the second term gives a vanishing contribution when multiplied by \not{p} in the trace. Hence, the differentiation with respect to n employed in the resummation technique removes a power of z . If further applying the eikonal approximation to the remaining fermion propagator,

$$\frac{\xi \not{p} - \not{l}}{(\xi p - l)^2} \gamma_\nu \not{p} \approx \frac{\xi \not{p}}{-2\xi p^+ v \cdot l} \gamma_\nu \not{p} = \frac{2\xi p^+ v_\nu}{-2\xi p^+ v \cdot l} \not{p} = -\frac{v_\nu}{v \cdot l} \not{p}, \quad (26)$$

Fig. 2 reduces to the second diagram in Fig. 1(b), and another power of z disappears.

We emphasize that the resummation technique is based on PQCD factorization theorems, and the factorization of the subdiagram makes sense only in the soft and hard regions. That is, the function $\bar{\phi}_s$, with the eikonal approximation, collects the leading contribution from the soft region $\xi \rightarrow x$, and $\bar{\phi}_h$ collects the leading contribution from the hard region. The subdiagram in Fig. 2, containing a finite piece of the splitting function, can not be absorbed into $\bar{\phi}_s$ or $\bar{\phi}_h$, since the quark propagator is not eikonalized, and the real gluon is not hard. Therefore, the finite part of the splitting function is completely missing in the resummation approach. In the conventional derivation of the DGLAP equation one-loop diagrams are computed explicitly without resort to eikonal (soft) approximation, and this makes the difference. The same conclusion applies to other cases that involve a soft approximation, such as the conventional derivation of the CCFM equation [3], where only the terms of the relevant splitting function singular at $z \rightarrow 1$ and at $z \rightarrow 0$ were reproduced, and the finite part was in fact put in by hand, as mentioned in Sect. IV.

III. THE BFKL EQUATION

In this section we demonstrate that the resummation technique reduces to the BFKL equation for the gluon distribution function in the small x region. The unintegrated gluon distribution function $F(x, k_T)$, defined by

$$F(x, k_T) = \frac{1}{p^+} \int \frac{dy^-}{2\pi} \int \frac{d^2 y_T}{4\pi} e^{-i(xp^+y^- - \mathbf{k}_T \cdot \mathbf{y}_T)} \times \frac{1}{2} \sum_{\sigma} \langle p, \sigma | F_{\mu}^+(y^-, y_T) F^{\mu+}(0) | p, \sigma \rangle, \quad (27)$$

in the axial gauge $n \cdot A = 0$, describes the probability of a gluon carrying a longitudinal momentum fraction x and transverse momenta \mathbf{k}_T . F_{μ}^+ is the field tensor. Similarly, we vary the vector n arbitrarily first to work out the resummation, and then show that the BFKL kernel is independent of n as in the DGLAP case. After deriving the evolution equation, n is brought back to the light cone.

We do not make explicit the p^+ dependence of F for the following reason. The BFKL equation governs the behavior of F with the momentum fraction x . The variation of x can be achieved by varying the hadron momentum p^+ , if the parton momentum $xp^+ = k^+$, appearing only in the exponent in Eq. (27), is fixed. Again, F involves the vectors k and n , which should combine into the ratio $(k \cdot n)^2/n^2$. Since k^+ is fixed, we do not choose it as an argument of F , and regard that F depends on p^+ implicitly through $x = k^+/p^+$. Hence, the derivative of F with respect to x is related to the derivative with respect to p^+ considered in the resummation formalism, and the chain rule in Eq. (4) holds:

$$-x \frac{d}{dx} F(x, k_T) = p^+ \frac{d}{dp^+} F(x, k_T) = -\frac{n^2}{v \cdot n} v_\alpha \frac{d}{dn_\alpha} F(x, k_T) . \quad (28)$$

Applying the operator d/dn to a gluon propagator, we get Eq. (5) and the same special vertex in Eq. (6). Summing all the diagrams with different differentiated gluons and employing the Ward identity, the special vertex moves to the outer end of the parton line as explained in Sect. II [4]. We then obtain the derivative of F ,

$$-x \frac{d}{dx} F(x, p_T) = 2\bar{F}(x, p_T) , \quad (29)$$

described by Fig. 3(a), where the new function \bar{F} contains one special vertex. It is easy to observe that Eq. (29) is the copy of Eq. (10) for the gluon distribution function.

We relate \bar{F} to F by factorizing out the subdiagram containing the special vertex, such that Eq. (29) reduces to a differential equation of F . In the leading soft and hard regions of l , which flows through the special vertex, the factorization is performed according to Figs. 3(b) and 3(c), respectively. Fig. 3(b) collects the soft divergences by eikonalizing the gluon propagator. We extract the color factor from the relation $f_{abc}f_{bdc} = -N_c\delta_{ad}$, where the indices a, b, \dots have been indicated in the figure, and $N_c = 3$ is the number of colors. The corresponding factorization formula is written as

$$\begin{aligned} \bar{F}_s(x, k_T) &= iN_c g^2 \int \frac{d^4 l}{(2\pi)^4} \Gamma_{\mu\nu\lambda} \hat{v}_\beta [-iN^{\nu\beta}(l)] \frac{-iN^{\lambda\gamma}(xp)}{-2xp \cdot l} \\ &\times \left[2\pi i \delta(l^2) F(x, |\mathbf{k}_T + \mathbf{l}_T|) + \frac{\theta(k_T^2 - l_T^2)}{l^2} F(x, k_T) \right] , \quad (30) \end{aligned}$$

where iN_c comes from the product of the overall coefficient $-i$ in Eq. (8) and the color factor $-N_c$ extracted above, and the triple-gluon vertex for vanishing l is given by

$$\Gamma_{\mu\nu\lambda} = -g_{\mu\nu}xp_\lambda - g_{\nu\lambda}xp_\mu + 2g_{\lambda\mu}xp_\nu . \quad (31)$$

The first term in the brackets corresponds to the real gluon emission, where $F(x, |\mathbf{k}_T + \mathbf{l}_T|)$ implies that the parton coming out of the hadron carries the transverse momenta $\mathbf{k}_T + \mathbf{l}_T$ in order to radiate a real gluon of momenta \mathbf{l}_T . The second term corresponds to the virtual gluon emission, where the θ function sets the upper bound of l_T to k_T to ensure a soft momentum flow.

It can be shown that the contraction of p with a vertex in the quark box diagram the partons attach, or with a vertex in the gluon distribution function, leads to a contribution down by a power $1/s$, $s = (p+q)^2$, compared to the contribution from the contraction with \hat{v}_β . Following this observation, Eq. (30) is expressed as

$$\begin{aligned} \bar{F}_s(x, k_T) = & iN_c g^2 \int \frac{d^4 l}{(2\pi)^4} N^{\nu\beta}(l) \frac{\hat{v}_\beta v_\nu}{v \cdot l} \left[2\pi i \delta(l^2) F(x, |\mathbf{k}_T + \mathbf{l}_T|) \right. \\ & \left. + \frac{\theta(k_T^2 - l_T^2)}{l^2} F(x, k_T) \right] , \end{aligned} \quad (32)$$

which corresponds to Fig. 3(b) exactly. The eikonal vertex v_ν comes from the last term divided by xp^+ in Eq. (31). The remaining metric tensor $g^{\mu\gamma}$ has been absorbed into F . Assuming $n = (n^+, n^-, \mathbf{0})$ for convenience, the integrations over l^- and l^+ to infinity in Eq. (32) give

$$\begin{aligned} \bar{F}_s(x, k_T) = & \frac{\bar{\alpha}_s}{2} \int \frac{d^2 l_T}{\pi} \frac{-n^2}{2n^- [n^+ l_T^2 + 2n^- l^+ + 2]} \Big|_{l^+=0}^{l^+=\infty} \\ & \times \left[F(x, |\mathbf{k}_T + \mathbf{l}_T|) - \theta(k_T^2 - l_T^2) F(x, k_T) \right] , \\ = & \frac{\bar{\alpha}_s}{2} \int \frac{d^2 l_T}{\pi l_T^2} \left[F(x, |\mathbf{k}_T + \mathbf{l}_T|) - \theta(k_T^2 - l_T^2) F(x, k_T) \right] , \end{aligned} \quad (33)$$

with $\bar{\alpha}_s = N_c \alpha_s / \pi$. The first line of the above formulas demonstrates explicitly how the n dependence cancels in the evaluation of Fig. 3(b).

The contribution from the first diagram of Fig. 3(c) is written as

$$\frac{\bar{\alpha}_s}{2} \int \frac{d^2 l_T}{\pi} \left[\frac{1}{l_T^2} - \frac{1}{l_T^2 + (k^+ \nu)^2} \right]$$

$$-\frac{1}{2} \frac{k^+ \nu}{[l_T^2 + (k^+ \nu)^2]^{3/2}} \ln \frac{\sqrt{l_T^2 + (k^+ \nu)^2} - k^+ \nu}{\sqrt{l_T^2 + (k^+ \nu)^2} + k^+ \nu} \Bigg] , \quad (34)$$

which confirms the statement that F depends on x (or p^+) via the ratio $(k \cdot n)^2/n^2 = (k^+ \nu)^2$. In the interesting region with small k^+ , Eq. (34) is less important (it vanishes as $k^+ \rightarrow 0$), and \bar{F}_s dominates. Ignoring the contribution from Fig. 3(c) along with its soft subtraction (the second diagram), that is, adopting $\bar{F} \approx \bar{F}_s$, Eq. (29) becomes

$$\frac{dF(x, k_T)}{d \ln(1/x)} = \bar{\alpha}_s \int \frac{d^2 l_T}{\pi l_T^2} \left[F(x, |\mathbf{k}_T + \mathbf{l}_T|) - \theta(k_T^2 - l_T^2) F(x, k_T) \right] , \quad (35)$$

which is exactly the BFKL equation. The n dependence residing in Fig. 3(c) is removed with the vanishing of Eq. (34) at small k^+ , and the BFKL kernel turns out to be gauge invariant. It is understood that the diagrams in Fig. 3(b) play the role of the BFKL kernel, a similar conclusion to that drawn at the end of Sect. II.

Since the explicit dependence of F on the large scale p^+ is neglected, the transverse degrees of freedom of a parton must be taken into account. This explains why the gluon distribution function at small x is constructed based on the high-energy k_T -factorization theorem [13]. Therefore, our formalism is applicable to the distribution functions defined according to the collinear factorization (the DGLAP case) and according to the k_T -factorization (the BFKL case).

IV. THE CCFM EQUATION

With the discussion in the previous two sections, it is not difficult to demonstrate that the resummation technique reduces to the CCFM equation, which embodies the DGLAP equation and the BFKL equation. It hints that we should maintain both the l^+ and l_T dependences in the unintegrated distribution function for the real gluon emission, namely, consider $F(x + l^+/p^+, |\mathbf{k}_T + \mathbf{l}_T|)$. The BFKL equation is appropriate for the multi-Regge region, where the transverse momenta carried by the rung gluons of a ladder diagram are of the same order, *i.e.*, $l_T \approx k_T$. Hence, the loop momentum l_T flowing through the distribution function is not negligible, and we can make

the soft approximation

$$F(x + l^+/p^+, |\mathbf{k}_T + \mathbf{l}_T|) \approx F(x, |\mathbf{k}_T + \mathbf{l}_T|) , \quad (36)$$

in \bar{F}_s , from which the BFKL equation is derived. While the DGLAP equation is appropriate for the transverse momentum ordered region, in which we have $l_T \ll p_T$, and thus the approximation

$$F(x + l^+/p^+, |\mathbf{k}_T + \mathbf{l}_T|) \approx F(x + l^+/p^+, k_T) . \quad (37)$$

The k_T dependence of the distribution function decouples, and is integrated out from both sides of Eq. (35). This is the reason a parton distribution function in the DGLAP equation needs not to involve the transverse degrees of freedom. The argument $x + l^+/p^+$ then leads to the splitting function. The same diagrams in Figs. 1(b) and 3(b) give the different evolution kernels, because they are factorized according to the different kinematic orderings of radiative gluons.

Start with

$$p^+ \frac{d}{dp^+} F(x, k_T, p^+) = 2\bar{F}(x, k_T, p^+) , \quad (38)$$

where the arguments k_T and p^+ of the unintegrated gluon distribution function manifest the attempt to unify the BFKL and DGLAP equations. Similarly, the new function \bar{F} involves one special vertex at the outer end of a parton line. If following the standard procedures of resummation, we should factorize out the subdiagram containing the special vertex in the leading soft and hard regions, and derive \bar{F}_s and \bar{F}_h , respectively, as in the previous sections. The function \bar{F}_h involves the lowest-order virtual gluon emission. This idea leads to a new unified evolution equation, which will be studied elsewhere [14]. To reproduce the CCFM equation, however, the inclusion of virtual gluons must be performed in a different way: They are embedded in \bar{F}_s , instead of absorbed into \bar{F}_h . Consequently, the factorization of the subdiagram is described by Fig. 4(a), where the two jet functions J group all-order virtual corrections, and the lowest-order real gluon emission between them is soft.

First, we resum the double logarithms contained in J by considering its derivative

$$\begin{aligned} p^+ \frac{d}{dp^+} J(p_T, p^+) &= \bar{J}(k_T, p^+) \\ &= [K_J(k_T, \mu) + G_J(p^+, \mu)] J(k_T, p^+) , \end{aligned} \quad (39)$$

which is similar to Eq. (17). At lowest order the function K_J comes from the first diagram of Fig. 3(b), and G_J from the two diagrams in Fig. 3(c). The relation between $K_J + G_J$ and J is simply multiplicative, since J collects only virtual gluons. We have set the infrared cutoff of K_J to k_T , as indicated by its argument. This cutoff is necessary here due to the lack of the corresponding real gluon emission, which serves as a soft regulator. The one-loop K_J can be obtained simply by working out the second integral in Eq. (32) without the θ function. The anomalous dimension of K_J is then found to be $\gamma_J = \bar{\alpha}_s$. The function G_J can also be computed, but its explicit expression is not important. The standard RG analysis leads to

$$K_J(k_T, \mu) + G_J(p^+, \mu) = - \int_{k_T}^{p^+} \frac{d\bar{\mu}}{\bar{\mu}} \gamma_J(\alpha_s(\bar{\mu})) , \quad (40)$$

with the initial conditions $K_J(k_T, k_T) = G_J(p^+, p^+) = 0$. Of course, we have neglected the constants of order unity in K_J and G_J .

Substituting Eq. (40) into (39), we solve for

$$J(k_T, Q) = \Delta(Q, k_T) J^{(0)} , \quad (41)$$

with the double-logarithm exponential

$$\Delta(Q, k_T) = \exp \left[-\bar{\alpha}_s \int_{k_T}^Q \frac{dp^+}{p^+} \int_{k_T}^{p^+} \frac{d\bar{\mu}}{\bar{\mu}} \right] . \quad (42)$$

We have chosen the upper bound of p^+ as Q , and ignored the running of $\bar{\alpha}_s$. The initial condition $J^{(0)}$ can be regarded as a tree-level gluon propagator, and then eikonalized in the evaluation of the soft real gluon emission below. We split the above exponential into

$$\Delta(Q, k_T) = \Delta_S^{1/2}(Q, zq) \Delta_{NS}^{1/2}(z, q, k_T) , \quad (43)$$

with $z = x/\xi$ and $q = l_T/(1-z)$, where ξ is the momentum fraction entering J from the bottom, and l_T is the transverse loop momentum carried by the real gluon. The so-called ‘‘Sudakov’’ exponential Δ_S and the ‘‘non-Sudakov’’ exponential Δ_{NS} are given by

$$\Delta_S(Q, zq) = \exp \left[-2\bar{\alpha}_s \int_{zq}^Q \frac{dp^+}{p^+} \int_{k_T}^{p^+} \frac{d\bar{\mu}}{\bar{\mu}} \right]$$

$$\begin{aligned}
&= \exp \left[-\bar{\alpha}_s \int_{(zq)^2}^{Q^2} \frac{dp^2}{p^2} \int_0^{1-k_T/p} \frac{dz'}{1-z'} \right] \\
\Delta_{NS}(z, q, p_T) &= \exp \left[-2\bar{\alpha}_s \int_{k_T}^{zq} \frac{dp^+}{p^+} \int_{k_T}^{p^+} \frac{d\bar{\mu}}{\bar{\mu}} \right] . \\
&= \exp \left[-\bar{\alpha}_s \int_z^{k_T/q} \frac{dz'}{z'} \int_{(z'q)^2}^{k_T^2} \frac{dp^2}{p^2} \right] , \tag{44}
\end{aligned}$$

where the variable changes $\bar{\mu} = (1 - z')p$ and $p^+ = p$ for Δ_S , and $\bar{\mu} = p$ and $p^+ = z'q$ for Δ_{NS} have been employed.

With Eq. (41), Fig. 4(a) reduces to Fig. 4(b), where the tree-level gluon propagator $J^{(0)}$ on the right-hand side has been eikonalized, and that of the left-hand side has been absorbed into F . Based on Fig. 4(b), \bar{F} is written as

$$\begin{aligned}
\bar{F}(x, k_T, p^+) &= iN_c g^2 \int \frac{d^4 l}{(2\pi)^4} N^{\nu\beta}(l) \frac{\hat{v}_\beta v_\nu}{v \cdot l} 2\pi i \delta(l^2) \Delta^2(Q, k_T) \\
&\quad \times \theta(Q - zq) F(x + l^+/p^+, |\mathbf{k}_T + \mathbf{l}_T|, p^+) . \tag{45}
\end{aligned}$$

Basically, the above formula is similar to the real gluon emission term in Eq. (32) except for the exponential Δ^2 from the two jet functions J , and the θ function. The θ function requires $Q > zq$ such that the Sudakov exponential Δ_S is meaningful, which comes from the angular ordering of radiative gluons $Q/(xp^+) > l_T/[(\xi - x)p^+]$. Compared with the transverse momentum ordering for the DGLAP equation [3, 15], $Q(l_T)$ has been divided by the gluon energy xp^+ ($(\xi - x)p^+$). Hence, the inserted scale zq reflects the special kinematic ordering for the CCFM equation. Those radiative gluons, which do not obey the angular ordering, contribute to the non-Sudakov exponential. This is one of the motivations to introduce the scale zq .

Using the variable change $\xi = x + l^+/p^+$ and performing the integration over l^- , we obtain

$$\begin{aligned}
\bar{F}(x, k_T, p^+) &= \frac{\bar{\alpha}_s}{2} \int_x^1 d\xi \int \frac{d^2 l_T}{\pi} \frac{2n^2(\xi - x)p^{+2}}{[n^+ l_T^2 + 2n^-(\xi - x)^2 p^{+2}]^2} \Delta^2(Q, k_T) \\
&\quad \times \theta(Q - zq) F(\xi, |\mathbf{k}_T + \mathbf{l}_T|, p^+) , \tag{46}
\end{aligned}$$

where $n = (n^+, n^-, \mathbf{0})$ has been assumed. Equation (46) is then substituted into (38) to find the solution of F . We integrate Eq. (46) from $p^+ = 0$ to Q , and adopt the variable changes $\xi = x/z$ and $\mathbf{l}_T = (1 - z)\mathbf{q}$. To work out the

p^+ integration, $F(x/z, |\mathbf{k}_T + \mathbf{l}_T|, p^+)$ is approximated by $F(x/z, |\mathbf{p}_T + \mathbf{l}_T|, l_T)$. The solution of F is given by

$$F(x, k_T, Q) = F^{(0)} + \bar{\alpha}_s \int_x^1 dz \int \frac{d^2 q}{\pi q^2} \theta(Q - zq) \Delta_S(Q, zq) \Delta_{NS}(z, q, k_T) \\ \times \frac{1}{z(1-z)} F(x/z, |\mathbf{k}_T + (1-z)\mathbf{q}|, l_T), \quad (47)$$

where the nonperturbative initial condition $F^{(0)}$ corresponds to the lower bound of p^+ . Again, the n dependence disappears for a similar reason to that for Eq. (33), and the CCFM kernel is gauge invariant.

Equation (47) can be reexpressed as

$$F(x, k_T, Q) = F^{(0)} + \int_x^1 dz \int \frac{d^2 q}{\pi q^2} \theta(Q - zq) \Delta_S(Q, zq) \tilde{P}(z, q, k_T) \\ \times F(x/z, |\mathbf{k}_T + (1-z)\mathbf{q}|, l_T), \quad (48)$$

with

$$\tilde{P} = \bar{\alpha}_s \left[\frac{1}{1-z} + \Delta_{NS}(z, q, k_T) \frac{1}{z} - 2 + z(1-z) \right], \quad (49)$$

which is close to the splitting function

$$P_{gg} = \bar{\alpha}_s \left[\frac{1}{1-z} + \frac{1}{z} - 2 + z(1-z) \right]. \quad (50)$$

Obviously, Eq. (48) is the CCFM equation [3]. To arrive at Eq. (49), we have employed the identity $1/(z(1-z)) \equiv 1/(1-z) + 1/z$, and put in by hand the last term $-2 + z(1-z)$. This term, finite at $z \rightarrow 0$ and at $z \rightarrow 1$, can not be obtained in the conventional approach either [3] as stated at the end of Sect. II. Note that only the non-Sudakov form factor Δ_{NS} in front of $1/z$ is kept, because Δ_{NS} vanishes when the upper bound zq of p^+ approaches zero, as shown in Eq. (44), and thus smears the $z \rightarrow 0$ pole of the function \tilde{P} . This is another motivation to introduce the scale zq . The above derivation shows that the complicated diagrammatic analysis involved in the conventional derivation of the CCFM equation [3] is avoided using the resummation technique.

VI. CONCLUSION

In this paper we have shown that the resummation technique provides a unified and simple viewpoint to the organization of the various large logarithms, and reduces to the DGLAP equation, the BFKL equation, and the CCFM equation in the different kinematic regions. The main idea is to relate the derivative of a parton distribution function to a new function involving a special vertex. The summation of the large logarithms is embedded in the new function without resort to complicated diagrammatic analyses. When expressing the new function as a factorization formula, we obtain the evolution equation. The subdiagram containing the special vertex, factorized according to the specific orderings of radiative gluons, leads to the corresponding kernels. By means of the resummation technique, the connection among the evolution equations becomes transparent.

Many applications of our formalism to small x physics follow this work, which will be briefly described below. In Eq. (30) associated with the BFKL equation, the real gluon emission term in fact involves the distribution function $F(x + l^+/p^+, |\mathbf{k}_T + \mathbf{l}_T|)$ as in the DGLAP and CCFM cases, instead of $F(x, |\mathbf{k}_T + \mathbf{l}_T|)$. The former is replaced by the latter when the strong rapidity ordering $x + l^+/p^+ \gg x$ *i.e.*, Eq. (36) is employed. Taking this into account, it is of no doubt that the loop momentum l^+ should not be extended to infinity in the derivation of Eq. (33), since $F(x + l^+/p^+)$ vanishes at large momentum fraction. If truncating l^+ at the scale of order Q , the resultant BFKL equation contains an intrinsic Q dependence. This modified equation has been proposed and studied in [16]. The HERA data of the DIS structure function $F_2(x, Q^2)$ [17], which exhibit a steep rise (corresponding to hard pomeron exchanges) at small x for large $Q^2 \sim 50 \text{ GeV}^2$, and a flat rise for low $Q^2 \sim 4 \text{ GeV}^2$ (because soft pomeron contributions begin to play), were explained successfully. Note that the Q dependence of the data can not be understood by means of the conventional BFKL equation.

Another consequence of relaxing the rapidity ordering is the recovery of the unitarity of the BFKL evolution. It can be easily recognized that real gluon emissions are responsible for the rise of the gluon distribution and the structure function F_2 . However, the approximation in Eq. (36) overestimates the real gluon contributions, such that F_2 rises as a power $x^{-\lambda}$, and violates the unitarity bound $F_2 \leq \text{const.} \ln^2(1/x)$. By adopting $F(x + l^+/p^+)$ in the evaluation of the BFKL kernel, we have been able to show that the power rise is moderated into a logarithmic rise [18]. The reason we have more freedom to modify the BFKL equation is that the gluons are not reggeized according

to the rapidity ordering before the BFKL kernel is derived.

The BFKL equation for the polarized gluon distribution function can be derived simply in our formalism [19]. After factorizing the subdiagram containing the special vertex, we contract Eq. (30) with the gluon polarization vectors $\epsilon_\mu \epsilon_\gamma$ for positive and negative helicities, and take their difference. The obtained equation will be employed to study the small x behavior of the polarized structure function $g_1(x)$, and may help to clarify the discrepancies between the previous and recent data of g_1 at $x \sim 10^{-2}$, and between the Regge extrapolation and the QCD fit for g_1 at $x \rightarrow 0$ [20].

It is well-known that the soft divergences from virtual and real radiative corrections to DIS cancel each other order by order. However, in the derivation of the CCFM equation virtual gluons are summed to all orders and grouped into the Sudakov and non-Sudakov form factors, while real gluon contributions are evaluated only to lowest order, which leads to the splitting function P_{gg} . To fulfill the soft cancellation, the coupling constant $\bar{\alpha}_s$ in the exponent of the Sudakov form factor Δ_S must be frozen, such that the lower bound q of the variable p^+ can reach zero, *i.e.*, $\Delta_S \rightarrow 0$ as shown in Eq. (44). The infrared singularity from the factor $1/q^2$ in the kernel of Eq. (48) is thus suppressed. Otherwise, a running $\bar{\alpha}_s(\bar{\mu})$ will prohibit q from being below Λ_{QCD} . However, the constant $\bar{\alpha}_s$ becomes a parameter. With our approach, it is trivial to derive a new unified evolution equation for the $\ln Q$ and $\ln(1/x)$ summations, in which both virtual and real corrections are considered to lowest order [14].

At last, to improve the accuracy of the kernel to next-to-leading logarithms, we only need to evaluate the $O(\alpha_s^2)$ subdiagram. Such an evaluation can be performed in a straightforward way. The BFKL equation including the summation of the next-to-leading $\ln(1/x)$ will be published elsewhere.

This work is supported by National Science Council of R.O.C. under the Grant No. NSC87-2112-M-006-018.

References

- [1] V.N. Gribov and L.N. Lipatov, Sov. J. Nucl. Phys. **15**, 428 (1972); G. Altarelli and G. Parisi, Nucl. Phys. **B126**, 298 (1977); Yu.L. Dokshitzer, Sov. Phys. JETP **46**, 641 (1977).
- [2] E.A. Kuraev, L.N. Lipatov and V.S. Fadin, Sov. Phys. JETP **45**, 199 (1977); Ya.Ya. Balitskii and L.N. Lipatov, Sov. J. Nucl. Phys. **28**, 822 (1978); L.N. Lipatov, Sov. Phys. JETP **63**, 904 (1986).
- [3] M. Ciafaloni, Nucl. Phys. **B296**, 49 (1988); S. Catani, F. Fiorani, and G. Marchesini, Phys. Lett. B **234**, 339 (1990); Nucl. Phys. **B336**, 18 (1990); G. Marchesini, Nucl. Phys. **B445**, 49 (1995).
- [4] J.C. Collins and D.E. Soper, Nucl. Phys. **B193**, 381 (1981).
- [5] H-n. Li, Phys. Rev. D **55**, 105 (1997).
- [6] H-n. Li, Phys. Lett. B **369**, 137 (1996).
- [7] G.P. Korchemsky, Mod. Phys. Lett. A **4**, 1257 (1989).
- [8] S. Catani and M. Ciafaloni, Nucl. Phys. **B236**, 61 (1984); **B249**, 301 (1985); S. Catani and M. Ciafaloni and G. Marchesini, Nucl. Phys. **B264**, 558 (1986).
- [9] J. Frenkel, J.G.M. Gatherall and J.C. Taylor, Nucl. Phys. **B233**, 307 (1984); J. Frenkel, P. Sorensen and J.C. Taylor, Z. Phys. C **35**, 361 (1987).
- [10] L.V. Gribov, E.M. Levin and M.G. Ryskin, Nucl. Phys. **B188**, 555 (1981); Phys. Rep. **100**, 1 (1983).
- [11] H-n. Li, Phys. Lett. B **405**, 347 (1997).
- [12] H-n. Li, in preparation.
- [13] T. Jaroszewicz, Acta. Phys. Pol. B **11**, 965 (1980); S. Catani, M. Ciafaloni, and F. Hautmann, Phys. Lett. B **242**, 97 (1990); Nucl. Phys. **B366**, 657 (1991); S. Catani and F. Hautmann, Nucl. Phys. **B427**, 475 (1994).

- [14] J.L. Lim and H-n. Li, in preparation.
- [15] J. Kwieciński, A.D. Martin, and P.J. Sutton, Phys. Rev. D **53**, 6094 (1996).
- [16] H-n. Li, Report No. NCKU-HEP-97-04, to appear in Phys. Lett. B.
- [17] ZEUS Collaboration, M. Derrick *et al.*, Z. Phys. C **65**, 379 (1995); H1 Collaboration, T. Ahmed *et al.*, Nucl. Phys. **B439**, 471 (1995).
- [18] H-n. Li, Report No. hep-ph/9709236.
- [19] H-n. Li and H.L. Yu, in preparation.
- [20] J. Lichtenstadt, presented at the International Symposium on QCD Corrections and New Physics, Hiroshima, Japan, 1997.

Figure Captions

FIG. 1. (a) The derivative $p^+ d\phi/dp^+$ in the axial gauge. (b) The soft structure and (c) the ultraviolet structure of the $O(\alpha_s)$ subdiagram containing the special vertex.

FIG. 2. One of the diagrams that contributes to the finite part of P_{qq} .

FIG. 3. (a) The derivative $-x dF/dx$ in the axial gauge. (b) The soft structure and (c) the ultraviolet structure of the $O(\alpha_s)$ subdiagram containing the special vertex.

FIG. 4. (a) The subdiagram containing the special vertex for the CCFM equation. (b) The subdiagram for the CCFM equation after resumming the double logarithms in J .

$$p^+ \frac{d}{dp^+} \left[\text{Diagram (a) Left} \right] = 2 \left[\text{Diagram (a) Right} \right]$$

(a)

$$\left[\text{Diagram (b) Left} \right] + \left[\text{Diagram (b) Right} \right]$$

(b)

$$\left[\text{Diagram (c) Left} \right] - \left[\text{Diagram (c) Right} \right]$$

(c)

FIG. 1

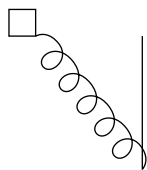
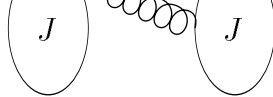


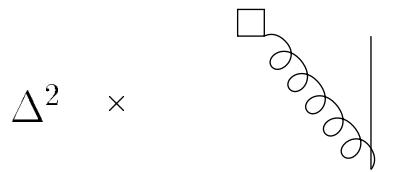
FIG. 2

$$\begin{array}{ccc}
-x \frac{d}{dx} & & 2 \\
\begin{array}{c} \text{diagram of } F \\ \text{with external lines } \gamma, \lambda c, \mu a, \nu b, \beta d \end{array} & = & \begin{array}{c} \text{diagram of } \bar{F} \end{array} \\
\text{(a)} & & \\
\begin{array}{c} \text{diagram of } F \\ \text{with external lines } \gamma, \lambda c, \mu a, \nu b, \beta d \end{array} & + & \begin{array}{c} \text{diagram of } \bar{F} \end{array} \\
\text{(b)} & & \\
\begin{array}{c} \text{diagram of } F \\ \text{with external lines } \gamma, \lambda c, \mu a, \nu b, \beta d \end{array} & - & \begin{array}{c} \text{diagram of } \bar{F} \end{array} \\
\text{(c)} & &
\end{array}$$

FIG. 3



(a)



(b)

FIG. 4